Optical-Electrical Characteristics and Carrier Dynamics of Semi-Insulation GaAs by Terahertz Spectroscopic Technique *

Xiao-Wei Han(韩小卫)[1,2], Lei Hou(侯磊)[1**], Lei Yang(杨磊)[1], Zhi-Quan Wang(王志全)[1], Meng-Meng Zhao(赵萌萌)[1], Wei Shi(施卫)[1**]

[1]*Department of Applied Physics, Xi'an University of Technology, Xi'an 710048*
[2]*Institute of Physical and Electrical Engineering, Weinan Normal University, Weinan 714000*

(Received 13 August 2016)

GaAs has been widely used to fabricate a variety of optoelectronic devices by virtue of its superior performance, and it is very important to accurately measure its electrical and optical properties. In this study, a semi-insulation (SI) GaAs wafer is investigated by the terahertz (THz) non-destructive testing technology. Using an air biased coherent generation and detection THz time domain spectroscopy system, the THz time domain waveform and spectrum of SI-GaAs are obtained by the time domain spectroscopy module, and its optical-electrical characteristics including complex refractive index, permittivity and dielectric loss angle are calculated. Its carrier lifetime is measured by the optical-pump THz-probe module, and the THz pulse induced intervalley scattering in photo-excited SI-GaAs is discussed.

PACS: 07.57.Ty, 78.20.Ci, 78.30.Fs DOI: 10.1088/0256-307X/33/12/120701

GaAs, as a second generation semiconductor material, has many superior performances including a wide energy gap, high electronic mobility, and large resistivity, thus it has been widely used to fabricate a variety of optoelectronic devices which can be operated at the conditions of high frequency, high voltage and high temperature.[1–4] Accurately measuring the optical-electrical properties and investigating the carrier dynamics of GaAs are very important to design and prepare GaAs high speed photoelectric devices. Some traditional methods have been used, such as the Hall-effect method[5,6] and the optical-pump-optical-probe (OPOP) method.[7] However, for the Hall-effect method, contact electrodes are required to be prepared on the wafer, thus the surface of the wafer is damaged. For the OPOP method, the probe laser beam can also excite electrons and holes in SI-GaAs, which will bring adverse effects to the results. Terahertz (THz) waves can partially penetrate and interact with GaAs, thus we can use the THz time-domain spectroscopic technique to detect the optical-electrical characteristics of GaAs nondestructively. Combining with the optical-pump-terahertz-probe (OPTP) method, we can obtain the dynamic behavior of photo-induced carriers. Although the THz spectroscopic technique has been used to measure GaAs and other semiconductors,[8,9] the spectral range is normally less than 3 THz. In this work, we measure SI-GaAs using an air biased coherent generation and detection THz time domain spectroscopy system, and the optical-electrical properties of SI-GaAs are obtained in the range of 1–6 THz. The carrier lifetime and nonlinear transient absorption bleaching are achieved by the OPTP method.

Figure 1 is the schematic diagram of the experimental setup of the air biased coherent generation and the detection THz time domain spectroscopy system with the OPTP module. An intense ultrafast laser pulse with a central wavelength of 800 nm, a time duration of 100 fs, a repetition rate of 1 kHz and a power of 5 W is generated by a regenerative laser amplifier (Spitfire, Spectra-Physics, USA) and the second harmonic pulse (400 nm) is generated by a nonlinear beta barium borate crystal (BBO). When the two pulses (400 nm and 800 nm) are collinearly focused into air, the intense THz pulses are emitted from the ionized air.[10] The THz pulses are detected in the gas plasma by the THz induced second harmonic,[11] which is measured by a photomultiplier tube (PMT), and its intensity is proportional to the THz electric field. THz time domain waveform can be mapped by moving stage 1 to change the relative delay between the THz pulses and optical probe pulses. SI-GaAs was placed in the focus of THz wave, and the whole system was purged by dry air.

For the OPTP module, stage 1 is fixed while the peak THz signal emerges, and then the time delay between the pump laser pulses and the THz pulses is changed by moving stage 2. The conductivity response of the sample after being excited by an optical

*Supported by the National Natural Science Foundation of China under Grant Nos 61575161 and 61427814, the National Basic Research Program of China under Grant No 2014CB339800, the Foundation of Shaanxi Key Science and Technology Innovation Team under Grant No 2014KTC-13, and the Special Financial Grant from the China Postdoctoral Science Foundation under Grant No 2013T60883.

**Corresponding author. Email: swshi@mail.xaut.edu.cn; houleixaut@126.com

© 2016 Chinese Physical Society and IOP Publishing Ltd

pulse can be recorded.

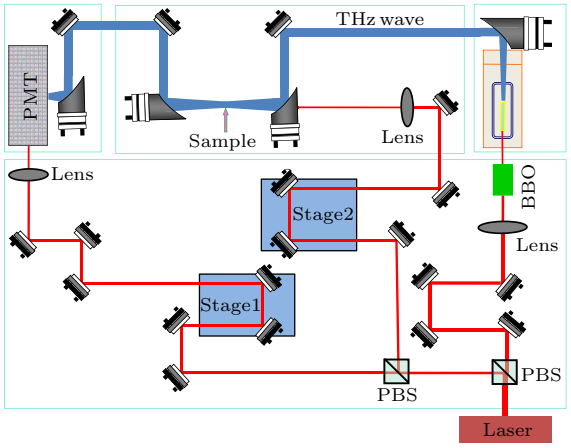

Fig. 1. Schematic diagram of the experimental setup of the air biased coherent generation and the detection THz time domain spectroscopy system with the OPTP module.

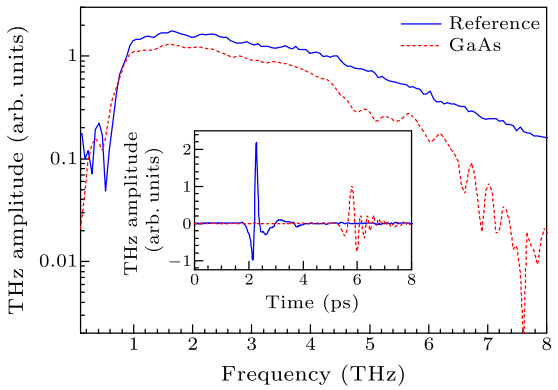

Fig. 2. THz spectra of reference (blue line) and the SI-GaAs sample (red line). The inset shows the corresponding time domain waveforms.

The inset of Fig. 2 shows the time domain waveforms of the reference THz pulse and the THz pulse propagated through the SI-GaAs sample, and their spectra can be obtained by the fast Fourier transform (FFT), as also shown in Fig. 2. It can be observed that the THz spectrum of the reference THz wave covers from 0.1 to more than 8 THz, while the transmission spectrum of the THz wave through the SI-GaAs ranges from 0.1 to about 6 THz due to the high frequency components absorbed by the SI-GaAs. Because the signal-to-noise ratio is low at the frequency of 0.1–1 THz, the results in this region are not accurate. In the following we discuss the results at the frequency of 1–6 THz.

Because the THz wave propagated in the SI-GaAs sample is dispersive and lossy, the parameters of the sample, including complex refractive index, absorption coefficient and electrical conductivity, all are the function of the frequency.[12] The complex refractive index can be used to characterize the macroscopic optical properties of the samples, and it can be expressed as

$$\tilde{n}(\omega) = n(\omega) - i\kappa(\omega), \tag{1}$$

where ω is the frequency, n is the real refractive index, and the imaginary part κ is the extinction coefficient. The expressions of n and κ are

$$n(\omega) = \varphi(\omega)c/\omega d + 1 \tag{2}$$

$$\kappa(\omega) = \ln\{4n(\omega)/\rho(\omega)[n(\omega)+1]^2\}c/\omega d, \tag{3}$$

where d is the sample thickness, c is the speed of light, and $\varphi(\omega)$ and $\rho(\omega)$ are the phase difference and the amplitude ratio of the sample beam and the reference beam, respectively.

Figure 3 shows the frequency dependence of the refractive index and the extinction coefficient of SI-GaAs, and the experimental results are represented by squared dots. As it can be seen from Fig. 3(a), the real part of the refractive index of SI-GaAs increases slightly as the frequency increases in the range of 1–6 THz, and the average refractive index is 3.71. The extinction coefficient reflects the absorption characteristics of the material. In Fig. 3(b), the extinction coefficient is large in the region with the frequency of 6–8 THz, and fluctuates below 0.02 m^{-1} between 1 and 6 THz. This means that THz waves acutely attenuate at the high frequency part, and they have a higher transmittance at 1–6 THz.

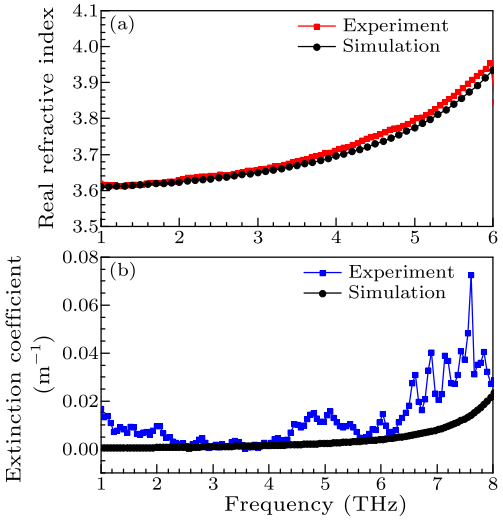

Fig. 3. (a) Frequency dependence of the refractive index of SI-GaAs. (b) Frequency dependence of the extinction coefficient of SI-GaAs.

The complex permittivity of the SI-GaAs sample can be expressed as $\tilde{\varepsilon} = \varepsilon_r + i\varepsilon_i$, the real part ($\varepsilon_r$) and the imaginary part (ε_i) are calculated by[13]

$$\varepsilon_r = n^2 - \kappa^2, \tag{4}$$

$$\varepsilon_i = 2n\kappa. \tag{5}$$

Figure 4 shows the frequency dependence of the complex permittivity of SI-GaAs, and the experimen-

tal results are represented by squared dots. The variation tendencies of $\varepsilon_{\rm r}$ and $\varepsilon_{\rm i}$ with frequency are the same as those of n and κ, which can be seen from Eqs. (4) and (5) under the condition of $\kappa \ll n$. Here $\varepsilon_{\rm r}$ increases from 13.09 to 15.64 with the frequency changing from 1 to 6 THz, which means that the material has a good dielectric property. The value of $\varepsilon_{\rm i}$ is very small in the range of 1–6 THz, thus the loss of THz waves in the SI-GaAs is weak and the material is a good candidate for the fabrication of THz devices.

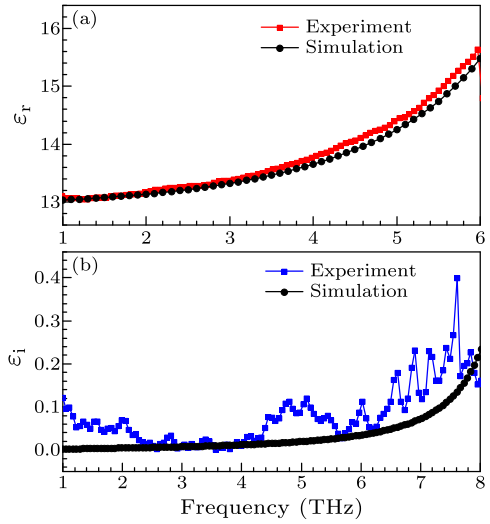

Fig. 4. (a) Frequency dependence of the real part of complex permittivity of SI-GaAs. (b) Frequency dependence of the imaginary part of complex permittivity of SI-GaAs.

In the engineering applications, the tangent of dielectric loss angle ($\tan\delta$) is usually used to describe the dielectric loss, which can be calculated by

$$\tan\delta = \kappa(\omega)/n(\omega). \tag{6}$$

Figure 5 shows the frequency dependence of the tangent of the dielectric loss angle of SI-GaAs, and the experimental results are represented by squared dots. When the frequency is larger than 1 THz, $\tan\delta$ is close to 0, which means that the dielectric loss of the SI-GaAs is weak.

The simulation results represented by round dots in Figs. 3–5 were obtained by the Lorentz dispersion model,[14] and the real part and the imaginary part of complex permittivity of GaAs can be expressed as

$$\varepsilon_{\rm r}(\omega) = \varepsilon_\infty + \frac{(\varepsilon_0-\varepsilon_\infty)(\omega_{\rm TO}^2-\omega^2)\omega_{\rm TO}^2}{(\omega_{\rm TO}^2-\omega^2)^2+\gamma^2\omega^2}, \tag{7}$$

$$\varepsilon_{\rm i}(\omega) = \frac{(\varepsilon_0-\varepsilon_\infty)\omega\gamma\omega_{\rm TO}^2}{(\omega_{\rm TO}^2-\omega^2)^2+\gamma^2\omega^2} \tag{8}$$

where ε_∞ is the high frequency dielectric constant, ε_0 is the low frequency dielectric constant, $\omega_{\rm TO}$ is the transverse optical phonon resonance frequency, and γ is the damping coefficient. Their values can be found in Ref. [15]. According to Eqs. (4) and (5), the real refractive index and the extinction coefficient are calculated by

$$n(\omega) = \sqrt{\frac{\varepsilon_{\rm r}(\omega)+\sqrt{\varepsilon_{\rm r}(\omega)^2+\varepsilon_{\rm r}(\omega)^2}}{2}}, \tag{9}$$

$$\kappa(\omega) = \sqrt{\frac{\sqrt{\varepsilon_{\rm r}(\omega)^2+\varepsilon_{\rm r}(\omega)^2}-\varepsilon_{\rm r}(\omega)}{2}}. \tag{10}$$

Comparing the results in Figs. 3–5, we can see that the experimental results match the simulation results very well for the real refractive index and the real part of the complex permittivity of SI-GaAs, and the variation tendencies of the experimental results and the simulation results are coincident for the extinction coefficient, the imaginary part of complex permittivity and the tangent of dielectric loss angle. Because Eqs. (7) and (8) are the first order approximation of the Lorentz dispersion model, and the experimental results are affected by tiny residual water in air, there are some deviations between the experimental results and the simulation results.

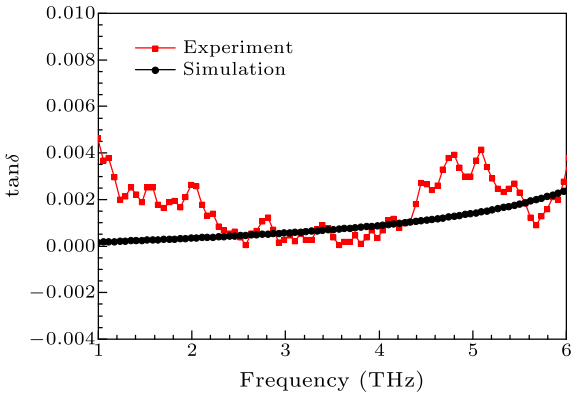

Fig. 5. Frequency dependence of the tangent of the dielectric loss angle of SI-GaAs.

In the OPTP system, the SI-GaAs wafer is placed at the focus of the THz probe beam and is photo-excited with a collinear pump beam with the wavelength of 800 nm and the time duration of 100 fs. The spot size diameters on the sample for the THz probe beam and the optical pump beam are 1.5 mm and 6 mm, respectively. The OPTP data are illustrated in Fig. 6, where the transmittance of THz wave from the SI-GaAs is recorded as a function of time following optical pump pulse excitation. The data are recorded with the optical gating beam at the maximum amplitude of the THz pulse, and the time axis refers to the pump-probe delay time obtained by scanning the optical beam delay stage 2. Reduced transmission of the probe beam occurs due to the pump induced SI-GaAs absorbance of THz waves by the photo generated carriers. This signal was detected in a double beam modulation scheme, in which both the pump beam and the THz source excitation beam were chopped. This step is necessary because the rectification

of the optical pump by the SI-GaAs sample causes a contaminating second THz pulse to be incident on the receiver.

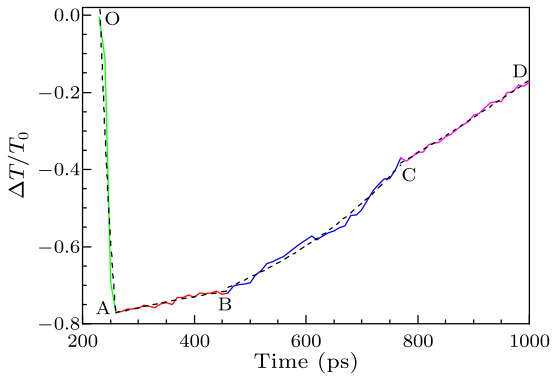

Fig. 6. The differential transmission optical-pump-THz-probe data of SI-GaAs, which includes the photo-excited carriers generating stage (OA), slow recombination process (AB), fast recombination process (BC) and slower recombination process (CD). The black dashed line is the fitting curve.

The OPTP curve can be divided into 4 stages labeled with OA, AB, BC and CD. The photo-excited carriers generated quickly in stage OA when the laser pulse illuminated on the SI-GaAs. Then, the photo-excited carriers underwent a slow recombination process (AB), fast recombination process (BC) and slower recombination process (CD). The process includes the recombination of electron-hole and the diffusion of electrons, and the former is predominant. The recombination of electron-hole is decided by auger recombination, defects recombination and radiative recombination, and the carrier lifetime can be theoretically calculated by[16]

$$1/\tau = 1/\tau_{\text{auger}} + 1/\tau_{\text{defect}} + 1/\tau_{\text{rad}}, \tag{11}$$

$$\tau_{\text{auger}} = 1/(N'^2 C_{\text{auger}}), \tag{12}$$

$$\tau_{\text{defect}} = 1/C_{\text{defect}}, \tag{13}$$

$$\tau_{\text{rad}} = 1/(N' C_{\text{rad}}), \tag{14}$$

where N' is carrier concentration, C_{auger}, C_{defect} and C_{rad} are the corresponding recombination rates, and their values are $7 \times 10^{-30}\,\text{cm}^6/\text{s}$, $5 \times 10^7/\text{s}$ and $1.7 \times 10^{-10}\,\text{cm}^3/\text{s}$, respectively. According to the equations, the theoretical carrier lifetime is 2.05 ns.

Table 1. Parameters of the fitting equation in stages AB, BC and CD.

i	t_i (ps)	A_i	y_i	RSS
AB	565.91	−0.301	−0.582	2.47×10^{-9}
BC	318.60	0.046	−0.899	1.42×10^{-8}
CD	1665.32	−0.916	0.184	3.66×10^{-9}

In Fig. 6, the exponential function ($Y_i = A_i \exp(-t/t_i) + y_i$) is used to fit the stages AB, BC and CD, and the fitting results are listed in Table 1. RSS is the residual sum of squares, and the values are very small, which means that the fitting degree is high. According to the fitting results, the carrier lifetime is 2.55 ns, which is close to the theoretical result.

By adjusting the laser power on the air plasma, we obtain the amplitude of the THz probe pulse at the sample corresponding to 'high THz field' and 'low THz field' conditions studied here with the peak electric fields of 153 kV/cm and 19 kV/cm, respectively, as estimated by[17]

$$E_0 = \sqrt{\frac{\eta_0 W}{\pi \omega_{\text{I}}^2 \int g^2(t) dt}}, \tag{15}$$

where E_0 is the THz peak electric field, η_0 is the free-space impedance, W is the THz energy, ω_{I} is the intensity beam waist, and $g(t)$ is the temporal shape of the THz electric field with a peak value normalized to 1. At the high THz field and low THz field, the pump powers of OPTP were adjusted to 5 mW, 10 mW and 15 mW, and we could measure the transmitted THz waveforms at the different delay times between the THz probe pulse and the pump pulse, and the results are shown in Figs. 7(a)–7(c). The dashed lines were measured at the delay time of −100 ps, which means that the THz probe pulse arrives at the sample ahead of the pump pulse and the sample is unexcited. The solid lines were measured at the delay time of 10 ps, which means that the THz probe pulse arrives at the sample behind the pump pulse and the sample is excited. Figure 7(d) is the transmittance of THz electric fields calculated by using the peak-to-peak value of THz pulse through an excited sample divided by that through the unexcited sample, and the red square dots and the blue round dots were measured at the low THz electric field and the high THz electric field, respectively. When the pump powers were 5 mW and 10 mW, the transmittance of THz wave with the high electric field was higher than that with the low electric field, which is called absorption bleaching. However, this phenomenon fades away with the increasing pump power.

The absorption bleaching observed at high THz probe fields is partially due to the THz-pulse-induced intervalley scattering of electrons between the Γ and L valleys in the GaAs conduction band.[18] Since the mobility of electrons in the L valley is much less than that in the central Γ valley, a high-field THz probe pulse that is able to induce intervalley scattering will effectively see less conductivity in the photo-excited SI-GaAs sample as compared with the low-field case where no intervalley scattering occurs. This results in an increase in transmission of the THz probe pulse at high THz fields. With increasing the pump power, the absorption bleaching fades away because the ratio of carriers, which experiences intervalley scattering, decreases with the increased concentration of photo-excited carriers. As the carriers population increases, the momentum component parallel to the THz E-field

vector is randomized due to the e–h scattering, limiting the maximum achievable velocity and hence the kinetic energy of the electrons.[19] The intervalley scattering rate depends on the energy of the electrons, thus it will be reduced at the high pump power.

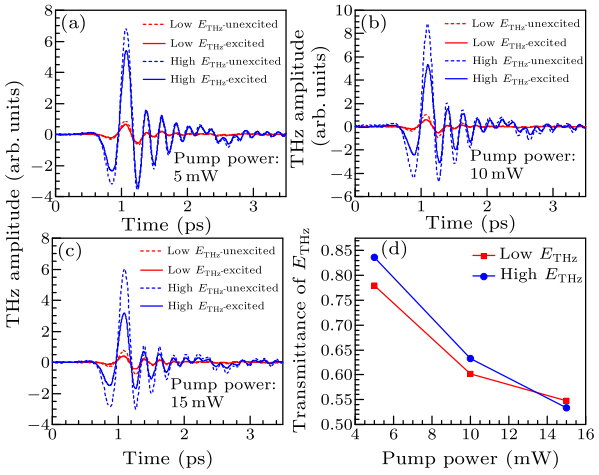

Fig. 7. Time domain waveforms of transmitted THz waves from unexcited and excited SI-GaAs at the low THz electric field and the high THz electric field with the pump powers of 5 mW (a), 10 mW (b) and 15 mW (c), and the transmittance of THz electric fields from SI-GaAs excited by different pump powers at the low THz electric field and the high THz electric field.

In summary, the performance of SI-GaAs has been comprehensively investigated by a non-destructive testing method based on the THz spectroscopic technique. The THz time domain waveform and spectrum of SI-GaAs are obtained by the time domain spectroscopy module, and its optical-electrical characteristics are calculated at 1–6 THz. The refractive index of SI-GaAs increases slightly as the frequency increases, and the average value is 3.71. The extinction coefficient is below 0.02 m^{-1} between 1 and 6 THz, which means that THz waves have a higher transmittance in this band. The value of ε_r increases from 13.09 to 15.64 with the frequency changing from 1 to 6 THz, which means that the material has a good dielectric property. Both ε_i and $\tan\delta$ illustrate that the loss of THz waves in the SI-GaAs is weak. The simulation results agree well with the experimental results. The carrier lifetime of SI-GaAs measured by the OPTP method is 2.55 ns, and the auger recombination, defects recombination and radiative recombination are the main influencing factors. The absorption bleaching is observed at high THz probe fields, which is in part due to the THz-pulse-induced intervalley scattering of electrons between Γ and L valleys in the GaAs conduction band, while the phenomenon fades away with the increasing pump power.

References

[1] Shi W, Tian L, Liu Z, Zhang L, Zhang Z, Zhou L, Liu H and Xie W 2008 *Appl. Phys. Lett.* **92** 043511
[2] Hou L, Shi W and Chen S 2013 *IEEE J. Sel. Top. Quantum Electron.* **19** 8401305
[3] Algora C, Ortiz E, Rey-Stolle I, Díaz V, Peña R, Andreev V M, Khvostikov V P and Rumyantsev V D 2001 *IEEE Electron Devices* **48** 840
[4] Wang C, Lee J and Kim N Y 2010 *Microwave Opt. Technol. Lett.* **52** 618
[5] Martin G M, Farges J P, Jacob G, Hallais J P and Poiblaud G 1980 *J. Appl. Phys.* **51** 2840
[6] Look D C 1990 *J. Electrochem. Soc.* **137** 260
[7] Hase M 2009 *Appl. Phys. Lett.* **94** 112111
[8] George P A, Strait J, Dawlaty J, Shivaraman S, Chandrashekhar M, Rana F and Spencer M G 2008 *Nano Lett.* **8** 4248
[9] Kadlec F, Nemec H and Kuzel P 2004 *Phys. Rev.* B **70** 125205
[10] Karpowicz N, Lu X and Zhang X C 2009 *J. Mod. Opt.* **56** 1137
[11] Dai J, Xie X, Zhang X C 2006 *Phys. Rev. Lett.* **97** 103903
[12] Han P and Zhang X C 2001 *Meas. Sci. Technol.* **12** 1747
[13] Bolivar P H, Brucherseifer M, Rivas J G, Gonzalo R, Ederra I, Reynolds A L, Holker M and Maagt P D 2003 *IEEE Trans. Microwave Theory Tech.* **51** 1062
[14] Sagor R H, Shahriar K A, Saber M G, Joy M A and Sohel I H 2016 *Silicon* **8** 251
[15] Palik E D 1985 *Handbook of Optical Constants of Solids* (San Diego: Academic Press)
[16] Strauss U, Rühle W W and Köhler K 1993 *Appl. Phys. Lett.* **62** 55
[17] Sharma G, Al-Naib I, Hafez H, Morandotti R, Cooke D G and Ozaki T 2012 *Opt. Express* **20** 18016
[18] Su F H, Blanchard F, Sharma G, Razzari L, Ayesheshim A, Cocker T L, Titova L V, Ozaki T, Kieffer J C, Morandotti R, Reid M and Hegmann F A 2009 *Opt. Express* **17** 9620
[19] Young J F, Kelly P J, Henry N L and Dharma-Wardana M W C 1991 *Solid State Commun.* **78** 343